Design of polarization-dependent, flexural-torsional deformation in photo responsive liquid crystalline polymer networks

Matthew L. Smith, Kyung Min Lee, Timothy J. White, Richard A. Vaia
October 4, 2013

Contents

1 Model Parameter Values

Parameters β, Q, and ν^{ph} were determined by fitting the model to bending data for monodomain strips fixed in cantilever configurations. All other model parameters were determined from experimental measurements. Monodomain parameters are in Table S1 and twisted nematic parameters are in Table S2.

Table S1 Monodomain model parameters used to fit model predictions of polarization dependent bending (tip angles) to the experimental data.

Parameter	Value	Description
a	$15\mu m$	strip thickness
b	$1mm$	strip width
L	$4.8mm$	strip length
I_o	$2mW/cm^2$	incident light intesity
$d_\parallel$	$3111nm$	atten. length ($\delta = 0°$)
$d_\perp$	$9837nm$	atten. length ($\delta = 90°$)
β	$-3.75\times10^{-5}cm^2\,mW^{-1}$	photocompliance
Q	0.45	order parameter
ν^{ph}	0.7	photo Poisson parameter

Table S2 Twisted nematic parameters used to fit model predictions of polarization dependent bending (tip angles) to the experimental data.

Parameter	Value	Description
a	$15\mu m$	strip thickness
b	$1mm$	strip width
L	$4.7mm$	strip length
I_o	$2mW/cm^2$	incident light intesity
$d_\parallel$	$3111nm$	atten. length ($\delta = 0°$)
$d_\perp$	$9837nm$	atten. length ($\delta = 90°$)
β	$-2.8\times10^{-5}cm^2\,mW^{-1}$	photocompliance
Q_o	0.75	order parameter ($x = \pm a/2$)
Q_i	0.45	order parameter ($x = 0$)
ν^{ph}	0.7	photo Poisson parameter

2 Attenuation Length

The attenuation length was obtained empirically. Representative data is shown in Fig. S1. See [White et al., *J. Mater. Chem.*, 2012, **22**, 691-698.] for experimental details.

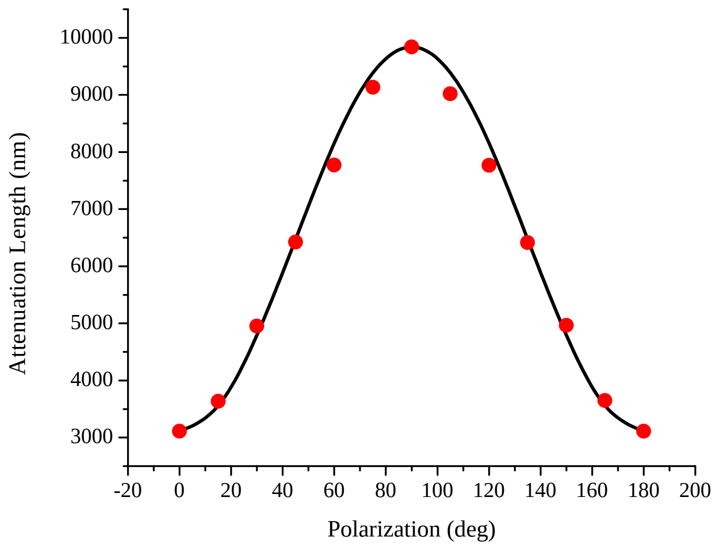

Fig. S1 Attenutation length for a representative monodomain sample using polarized light. The length here is obtained by taking the natural logarithm of the difference in incident intensity and transmitted intensity and solving for d.

3 Monodomain Flexure and Torsion Surface Plots

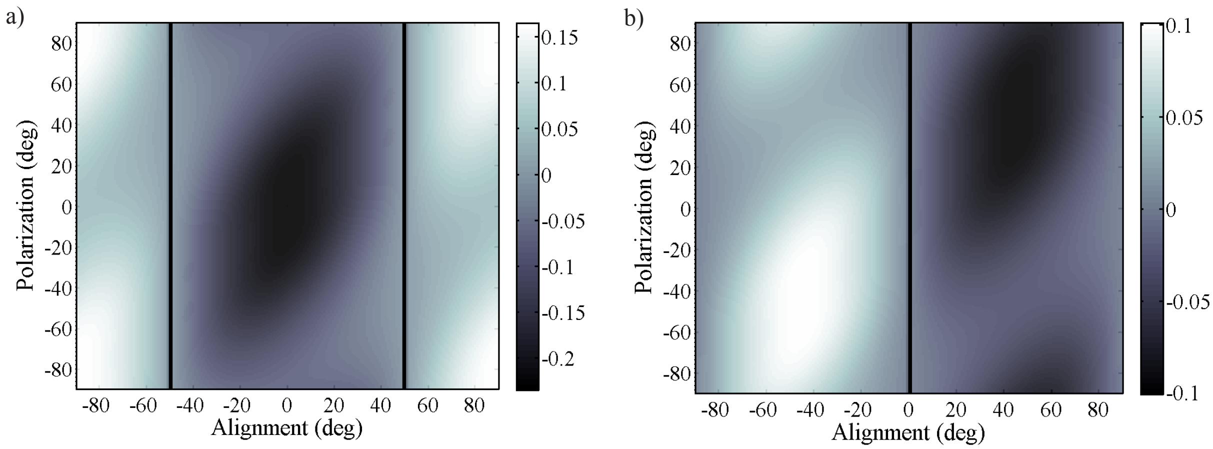

Fig. S2 (a) Bending curvature and (b) twist per length for a monodomain strip as a function of polarization and alignment. Black lines show zero curvature or twist, respectively. Curvature and twist units are mm^{-1}. There is also a line of zero twist at the $\pm 90^{\circ}$ alignment.

4 Additional Neutral Surface Plots

Figure S3 gives additional representative samples of computed normal and shear strains.

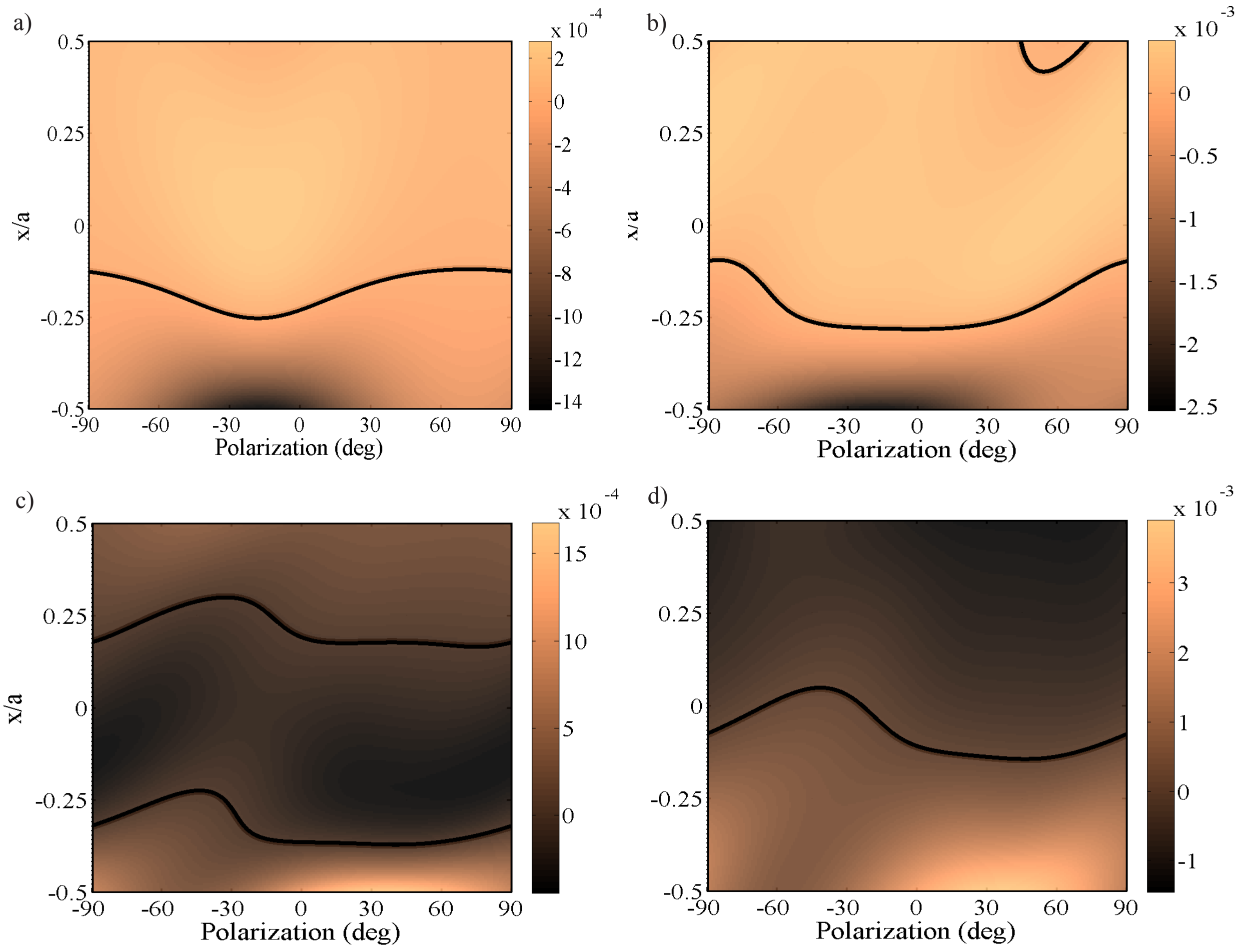

Fig. S3 Strain as a function of polarization and depth throughout the film thickness. (a) Computed shear strain in a monodomain strip with alignment $\theta_o = -\pi/10$. (b) Computed shear strain in a twisted nematic strip with alignment $\theta_o = -\pi/10$. (c) Computed normal strain in a twisted nematic strip with alignment $\theta_o = \pi/5$. (d) Computed shear strain in a twisted nematic strip with alignment $\theta_o = \pi/5$.

5 Selected Configurations

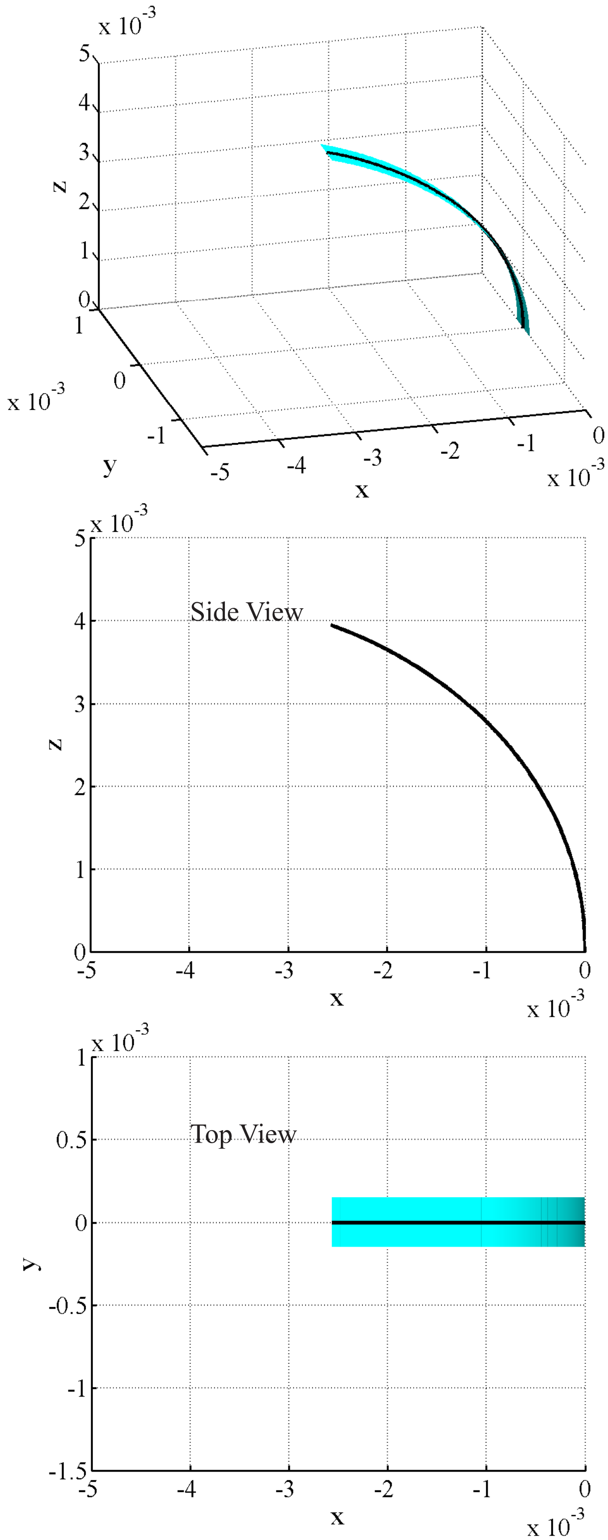

Fig. S4 Predicted configuration of a monodomain azo-LCN strip with 0° alignment and 0° polarization. The black line is the centerline. A 5mm long strip is shown. The width for computation was $b = 150\mu m$. All axes units are m.

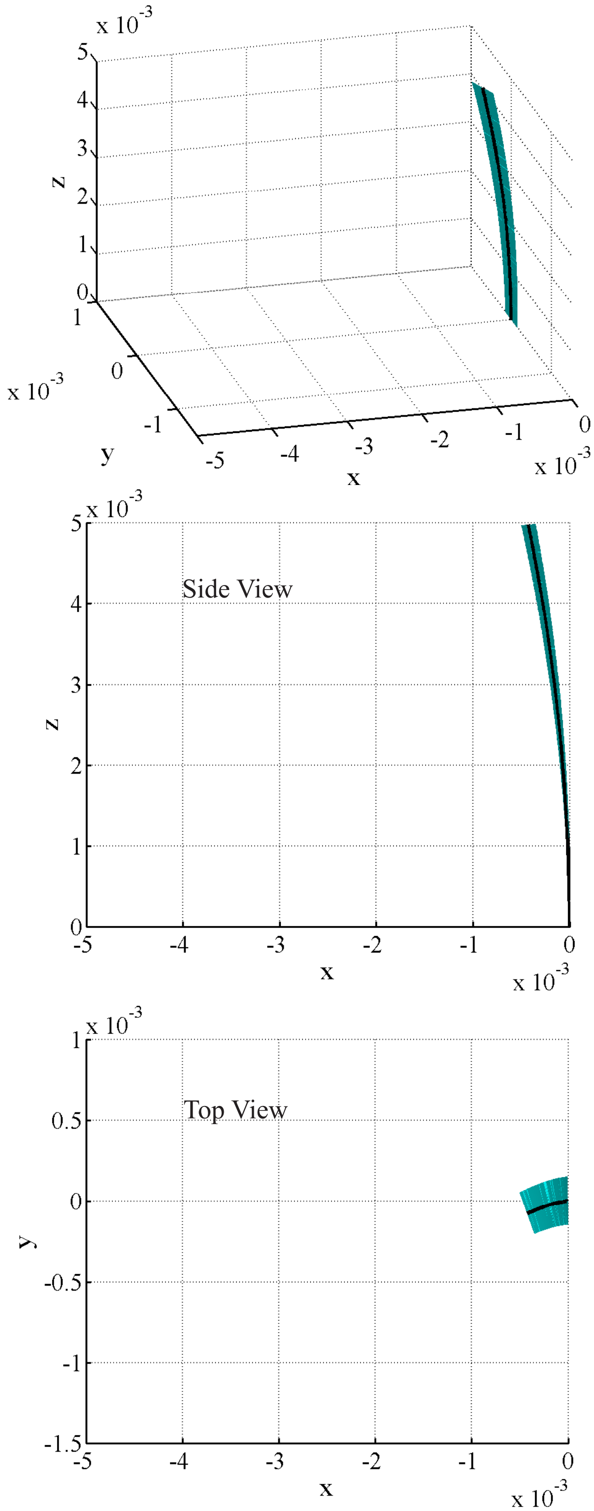

Fig. S5 Predicted configuration of a monodomain azo-LCN strip with -45° alignment and -45° polarization. $L = 5mm$, $b = 150\mu m$.

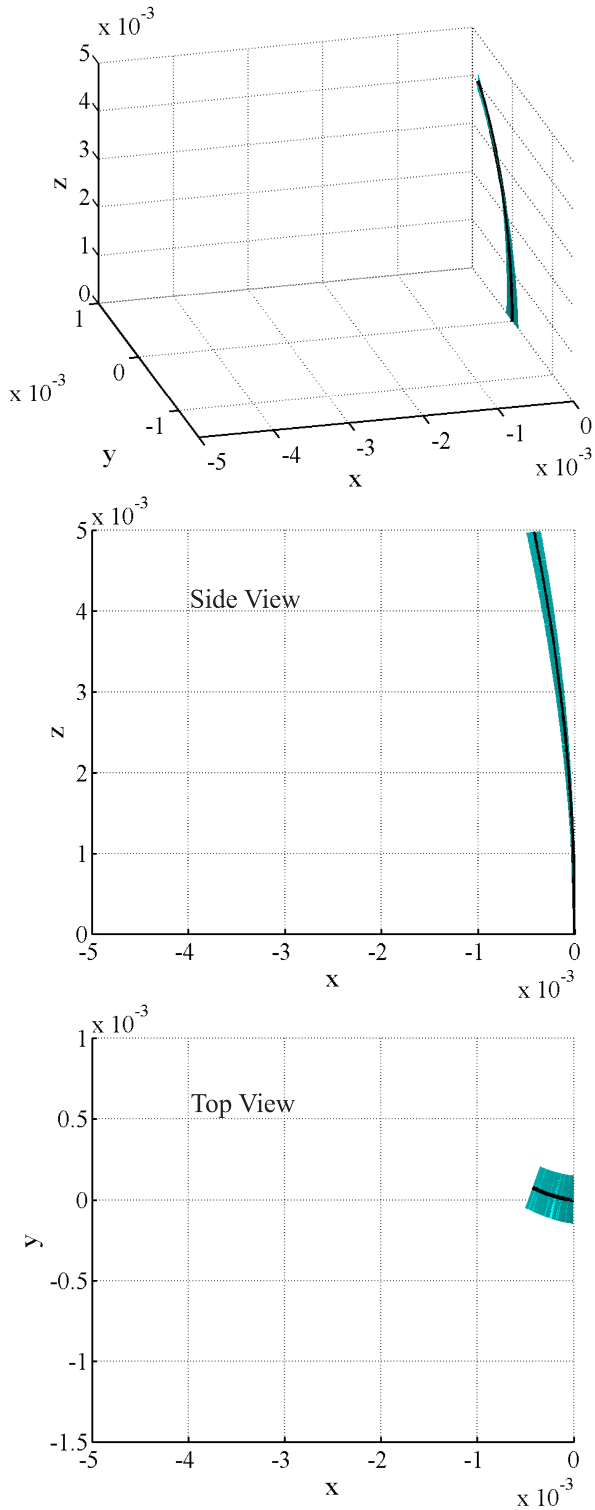

Fig. S6 Predicted configuration of a monodomain azo-LCN strip with 45° alignment and 45° polarization. $L = 5mm$, $b = 150\mu m$.

6 Finite Element Modeling

Here we briefly present a basic finite element prediction of monodomain azo-LCNs with alignments of 0°, −45°, and 45°. In all cases $\theta_o = \psi$. We follow the approach of Dunn in modeling the photo induced deformation parallel to the material alignment via an analogous bilayer in which one layer undergoes a uniform change in natural length. [Dunn, M.L. *J. Appl. Phys.* 2007, **102**, 013506]. The appropriate layer thickness and uniform contraction are determined by first calculating the integrals associated with the normal force on a cross section and the moment about the y-axis direction (see the first two sub-equations in the left column of Eq. (9) in the main text) for both the exponential light case and the bilayer case. Then the results of the two normal force integrals are equated and the results of the two moment integrals are equated. The thickness and uniform contraction strain can be solved for in terms of the original model parameters. To apply the uniform strain at different angles we simply created a composite layer structure with one layer having orthotropic coefficients of thermal expansion and the other layer being impervious to temperature. The simulations were performed using the commercial finite element software Abaqus. The thickness of the responsive layer was $5.98\mu m$ and the total thickness was $15\mu m$. The applied uniform strain parallel to the material alignment was -0.00245 and the perpendicular strain was -0.7 of this quantity. Young's modulus was set to $1GPa$ and the Poisson ratio was set to $\nu = 0.35$. One edge of the strip was fix against all rotations and translations. In comparing the finite element and analytical model for the $150\mu m$ wide strips the flexural torsional deflections agree very well qualitatively for alignments set to 0°, −45°, and 45° (compare Figures S4, S5, and S6 and Figures S7 and S8). Horizontal deflections at the tip are given in Table S3. Here the value are of the right order of magnitude, but vary quantitively by up to 34%. Reasons for this variation include the applied boundary conditions in the finer element model versus the free film in the analytical model. In addition, the finite element model can better account for competition between bending and twisting modes. Figure S9 and Figure S10 show deformed configurations for $1mm$ wide strips predicted by the finite element method.

Table S3 Horizontal tip deflections (in the finite element model this is the z direction) away from the straight configuration as predicted by the analytical model and the finite element simulations.

Alignment	Analytical	Finite Element
0°	$2.55mm$	2.08 mm
45°	$0.42mm$	0.64 mm
−45°	$0.42mm$	0.64 mm

6.1 Strips with Width 150μm

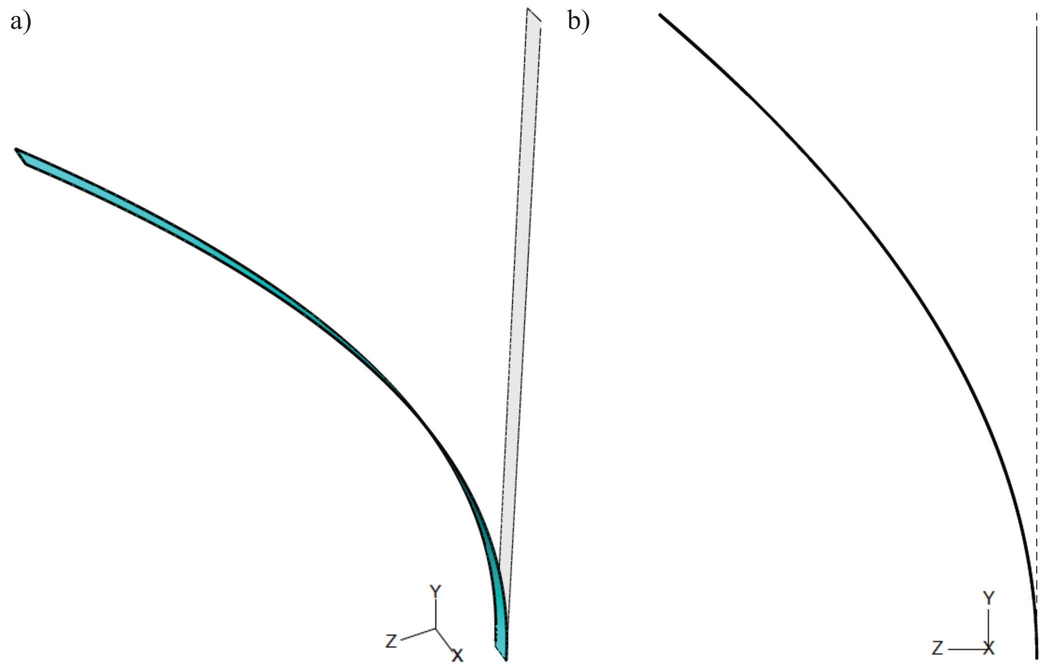

Fig. S7 FE predicted configuration of a monodomain azo-LCN strip with 0° alignment and 0° polarization. $L = 5mm$, $b = 150\mu m$. (a) Isometric view. (b) Side view. The straight, undeformed configuration is also shown.

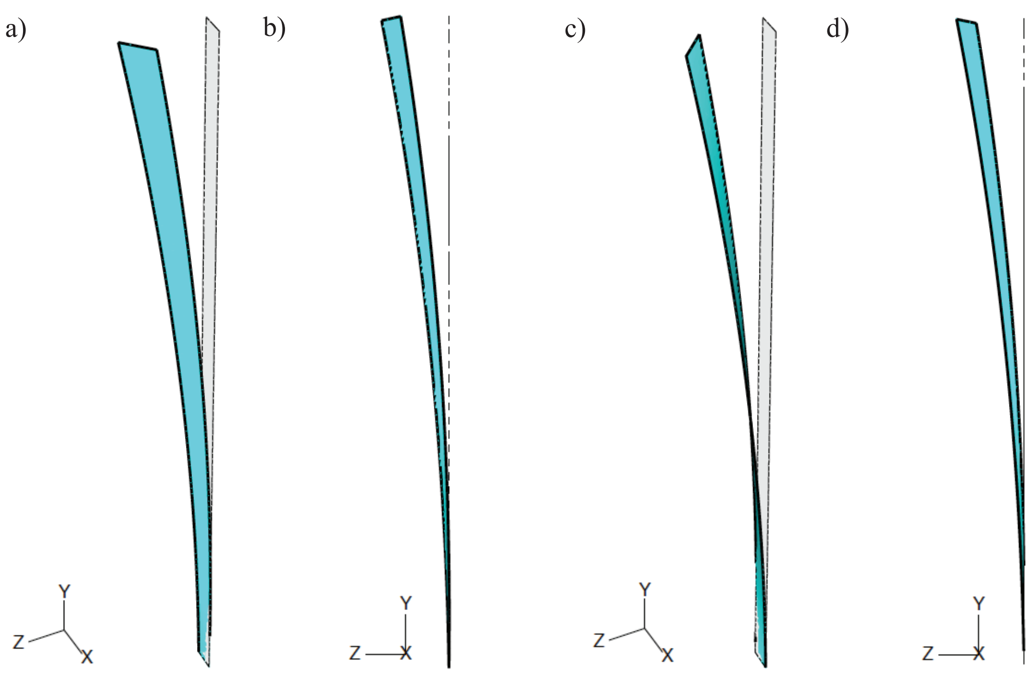

Fig. S8 FE predicted configuration of a monodomain azo-LCN strip with (a,b) $-45°$ alignment and $-45°$ and (c,d) 45° alignment and 45° polarization. $L = 5mm$, $b = 150\mu m$. Side views are given in (b) and (d).

6.2 Strips with Width 1mm

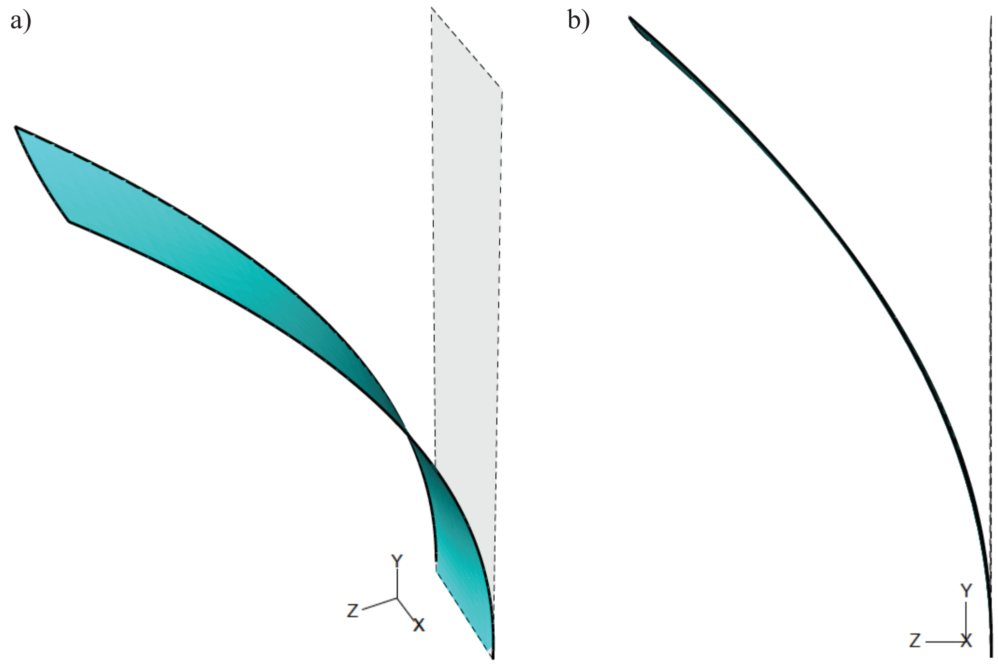

Fig. S9 FE predicted configuration of a monodomain azo-LCN strip with 0° alignment and 0° polarization. $L = 5mm$, $b = 1mm$. (a) Isometric view. (b) Side view.

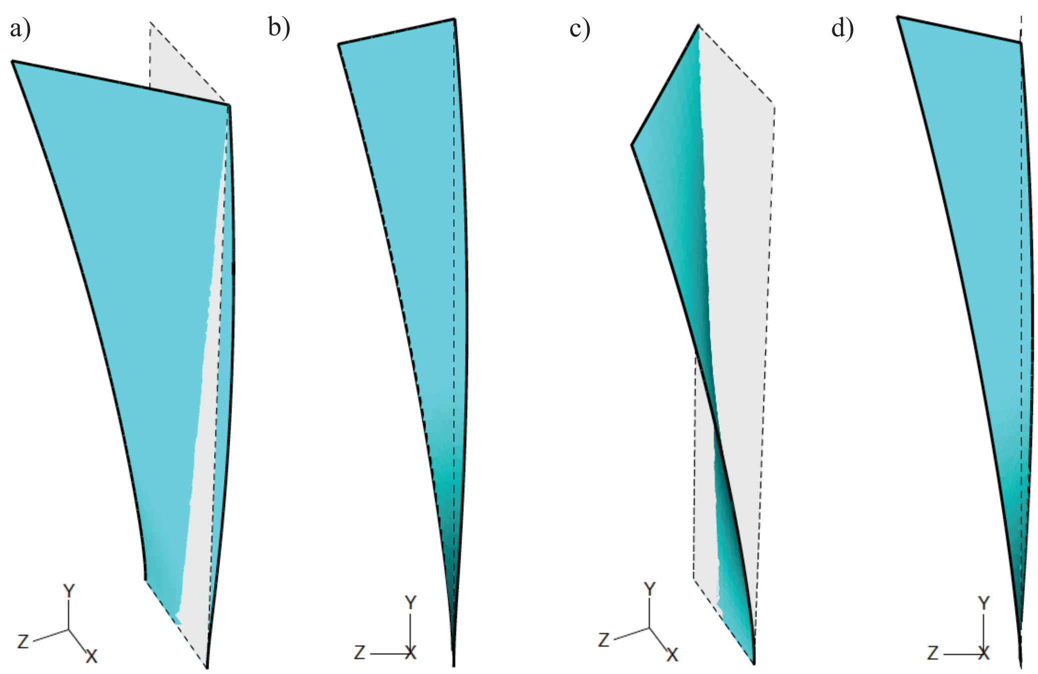

Fig. S10 FE predicted configuration of a monodomain azo-LCN strip with (a,b) −45° alignment and −45° and (c,d) 45° alignment and 45° polarization. $L = 5mm$, $b = 1mm$. Side views are given in (b) and (d).